Submitted to *Journal Geophysical Research* 01/19/1999 – in press, October 1999

Chemical NO_x budget in the upper troposphere over the tropical South Pacific

Martin G. Schultz,[1,2] Daniel J. Jacob,[1] John D. Bradshaw,[3] Scott T. Sandholm,[4] Jack E. Dibb,[5] Robert W. Talbot,[5] and Hanwant B. Singh[6]

Abstract

The chemical NO_x budget in the upper troposphere over the tropical South Pacific is analyzed using aircraft measurements made at 6-12 km altitude in September 1996 during the Global Tropospheric Experiment (GTE) Pacific Exploratory Mission (PEM) Tropics A campaign. Chemical loss and production rates of NO_x along the aircraft flight tracks are calculated with a photochemical model constrained by observations. Calculations using a standard chemical mechanism show a large missing source for NO_x; chemical loss exceeds chemical production by a factor of 2.4 on average. Similar or greater NO_x budget imbalances have been reported in analyses of data from previous field studies. Ammonium aerosol concentrations in PEM-Tropics A generally exceeded sulfate on a charge equivalent basis, and relative humidities were low (median 25% relative to ice). This implies that the aerosol could be dry in which case N_2O_5 hydrolysis would be suppressed as a sink for NO_x. Suppression of N_2O_5 hydrolysis and adoption of new measurements of the reaction rate constants for $NO_2 + OH + M$ and $HNO_3 + OH$ reduces the median chemical imbalance in the NO_x budget for PEM-Tropics A from 2.4 to 1.9. The remaining imbalance cannot be easily explained from known chemistry or long-range transport of primary NO_x and may imply a major gap in our understanding of the chemical cycling of NO_x in the free troposphere.

1. Introduction

Reactive nitrogen oxides ($NO_x = NO + NO_2 + NO_3 + 2\ N_2O_5 + HNO_2 + HO_2NO_2$) play a critical role in the photochemical production of ozone in the troposphere, and they have a major effect on the abundance and partitioning of HO_x radicals ($= OH +$ peroxy species) which determine the oxidizing power of the troposphere. Sources of NO_x in the tropical upper troposphere include major contributions from convective input of NO_x emitted at the surface, chemical recycling from nitric acid (HNO_3) and peroxyacetylnitrate (PAN) and production from N_2 and O_2 in lightning flashes. The residence time of air in the tropical upper troposphere is about 10 days [*Prather and Jacob*, 1997]. This is generally long compared to the lifetime of NO_x with respect to oxidation to the reservoir species HNO_3 and PAN (2–10 days [*Jacob et al.*, 1996]). Therefore one would expect average NO_x concentrations in the upper troposphere to be near a chemical steady state between loss by oxidation and recycling from the reservoirs.

The most important NO_x reservoir in the upper troposphere according to current models is HNO_3. HNO_3 is formed during daytime through oxidation of NO_2 by OH and during nighttime by hydrolysis of N_2O_5 on aqueous aerosol surfaces (N_2O_5 itself is formed by reaction of NO_2 with NO_3, where NO_3 is produced by reaction of O_3 with NO_2). Regeneration of NO_x from HNO_3 takes place during daytime by photolysis and reaction with OH. Conversion of NO_x to PAN in the upper troposphere takes place by photochemical degradation of acetone and other carbonyls [*Singh et al.*, 1995]. PAN is photolyzed back to NO_x (thermal decomposition of PAN is very slow in the upper troposphere). The cycling between NO_x and PAN in the tropical upper troposphere is typically 10 times slower than the cycling between NO_x and HNO_3 [*Jacob et al.*, 1996].

Observed $HNO_3/(NO + NO_2)$ concentration ratios (hereinafter denoted as R_N) in the free troposphere can be compared to chemical steady state model calculations as a test of the cycling between NO_x and HNO_3 [*Chatfield*, 1994]. Model ratios reported in a number of studies overestimate observed values by factors of 2-10 [*Liu et al.*, 1992; *Chatfield*, 1994; *Davis et al.*, 1996; *Hauglustaine et al.*, 1996; *Jacob et al.*, 1992, 1996; *Jaeglé et al.*, 1998] suggesting major flaws in our current understanding of the chemical budget of NO_x. Similar overestimates are found in global three-dimensional models [*Brasseur et al.*, 1996; *Wang et al.*, 1998a,b; *Lawrence and Crutzen*, 1998; *Hauglustaine et al.*, 1998]. Only a few studies find no discrepancy [*Fan et al.*, 1994; *Singh et al.*, 1998].

It has been proposed that the overestimate of R_N in chemical models is due to a perturbation of the chemical equilibrium by primary NO_x sources from lightning, aircraft, or deep convection [*Singh et al.*, 1996b; *Liu et al.*, 1996; *Smyth et al.*, 1996; *Kawakami et al.*, 1997; *Prather and Jacob*, 1997; *Jaeglé et al.*, 1998]. *Prather and Jacob* [1997] used a simple box model to determine the mean shift in upper tropospheric (above 12 km altitude) R_N due to tropical deep convection. With a dynamical turnover rate of 10%/day and a chemical lifetime of NO_x of 10 days, they find that injection of primary NO_x from convection and lightning would lower R_N by a factor of 2 from its chemical equilibrium value. The effect would be less at lower altitudes because of the shorter lifetime of NO_x. In an analysis of aircraft data (8-12 km) over the central United States, *Jaeglé et al.* [1998] found that the discrepancy between simulated and observed $NO_y/(NO + NO_2)$ ratios ($NO_y = NO_x + HNO_3 +$ organic nitrates) was anticorrelated with the number concentration of condensation nuclei. They concluded that convective injection of boundary layer NO_x plays an important role in lowering R_N.

Other investigations have attempted to explain the model overestimates of R_N by invoking a fast chemical reaction to convert HNO_3 to NO_x in sulfate aerosols [*Chatfield*, 1994; *Fan et al.*, 1994] or on soot [*Hauglustaine et al.*, 1996; *Lary et al.*, 1997]. However, there is so far no laboratory evidence for fast conversion of HNO_3 to NO_x under conditions representative of the upper tropospheric aerosol [*Jacob*, 1999].

We present in this paper a chemical model analysis of airborne observations made up to 12 km altitude over the remote tropical and subtropical South Pacific in September 1996 (PEM-Tropics A [*Hoell et al.*, 1999]). This study extends the brief discussion of the chemical NO_x budget given by *Schultz et al.*[1999] in light of new kinetic data and information on aerosol composition. A review of previous studies is also presented.

2. Chemical NO_x Budget During PEM-Tropics A

The Global Tropospheric Experiment (GTE) Pacific Exploratory Mission (PEM) Tropics A campaign [*Hoell et al.*, 1999] surveyed the troposphere over the South Pacific in September and October 1996, during the peak of the burning season in the Southern Hemisphere. Two aircraft, a DC-8 and a P-3B, each spent more than 120 hours in flight conducting extensive trace gas measuremements. In this paper we focus on data from the DC-8 aircraft because it had a higher ceiling (12 km compared to 8 km for the P-

3B) and there were no HNO_3 measurements on board the P-3B. We restrict our analysis to the tropical and subtropical South Pacific (0–30°S, 165°E–105°W) and to altitudes above 6 km. The aircraft data are averaged over the HNO_3 measurement intervals (∼3 min), which were the longest of all the gas-phase species observed. This data set is then used to constrain the chemical model. For the discussion of the aerosol chemical composition in section 3, the temporal resolution of the aerosol measurements ($\sim$ 20 min) is retained.

Figure 1 shows vertical profiles for the mixing ratios of several NO_y species over the tropical South Pacific during PEM-Tropics A. NO_x was computed from the sum of observed NO (measured with two-photon laser induced fluorescence (TP-LIF) [*Bradshaw et al.,* 1985; *Sandholm et al.,* 1990, 1994, 1997]) and locally computed chemical model values for NO_2, HO_2NO_2, NO_3, and N_2O_5 [*Schultz et al.,* 1999]. *Schultz et al.* [1999] compared observed and modeled NO_2/NO ratios and found agreement to within 30% (interquartile range) at all altitudes above 2 km. We will use calculated NO_2 throughout the remainder of this paper because of the greater availability. HNO_3 was measured with the mist chamber technique [*Talbot et al.,* 1988, 1990, 1997], and PAN was measured with a gas chromatography electron capture detector (GC/ECD) system [*Singh and Salas,* 1983; *Gregory et al.,* 1990a]. Table 1 compiles the instrumental accuracies and limits of detection (LOD) for the key NO_y species during PEM-Tropics A.

Concentrations of PAN and HNO_3 show pronounced maxima in the lower and middle free troposphere (between 2 and 8 km), reflecting the extensive biomass burning influence during PEM-Tropics A [*Schultz et al.,* 1999; *Talbot et al.,* 1999a]. Concentrations of NO_x increase steadily with altitude, reaching typical values of 50 parts per trillion by volume (pptv) at 8-10 km (Figure 1b). The observed R_N is about 5 mol/mol in the lower and middle troposphere and decreases to 1 mol/mol at 8 km and to about 0.4 mol/mol at 11 km (Figure 1e). The median NO/NO_x ratio (not shown) above 6 km is 0.53 (interquartile range 0.47-0.58) for zenith angles $< 60°$. Figure 1f displays the concentration ratio of aerosol nitrate (NO_3^-) to gas-phase HNO_3. Aerosol nitrate was measured from bulk filter samples [*Dibb et al.,* 1999]. The median NO_3^-/HNO_3 ratio at 6-12 km is 0.29 mol/mol, and the interquartiles span the range from 0.15 to 0.91 mol/mol. Of the NO_3^- data above 6 km, 55% are below the limit of detection (10 pptv). In marine convective outflow, NO_3^- concentrations occasionally exceeded gas-phase HNO_3 concentrations by up to a factor of 4.

Table 2 gives medians and interquartile ranges for the air mass composition over the tropical and subtropical South Pacific at 6–12 km altitude. The subset of data with very low relative humidity ($< 10\%$) exhibits significantly enhanced pollution presumably from biomass burning (compare concentrations of CO, C_2H_2, PAN, and organic acids of this subset with the overall data). While the lower R_N and higher C_2H_2/CO ratio indicate relatively fresh pollution in these air masses, the high concentrations of HNO_3 and organic acids suggest that they have not encountered scavenging in convection for at least a couple of days.

We calculated chemical production and loss rates of NO_x along the PEM-Tropics A DC-8 flight tracks with a chemical point model [*Schultz et al.,* 1999]. The model is constrained by concurrent observations of O_3, HNO_3, PAN, H_2O, CO, H_2O_2, CH_3OOH, hydrocarbons, temperature, and photolysis frequencies for NO_2 and for O_3 to $O(^1D)$. The NO_x concentration is chosen so that the model NO reproduces the observed NO within 1% at the solar time of measurement. The model computes local HO_x concentrations and chemical rates in diurnal steady state, defined by repeatability of model results over a 24 hour solar cycle. Acetone was not measured, and a typical concentration of 400 pptv was assumed [*Singh et al.,* 1995; *McKeen et al.,* 1997]. Our results are only modestly sensitive to this assumption (a 30% decrease in the acetone concentration leads to a 10% improvement in the chemical NO_x budget imbalance). The standard gas-phase chemical mechanism of the model follows the recommendations of JPL-97 [*DeMore et al.,* 1997], completed for volatile organic compound chemistry by *Atkinson et al.* [1997]. Absorption cross sections and quantum yields for photolysis of acetone are from *Gierczak et al.* [1998].

Heterogeneous oxidation of NO_x to HNO_3 is described as first-order losses of N_2O_5 and NO_3 on aerosol surfaces. Reaction probabilities follow the recommendations of *Jacob* [1999], i.e. $\gamma = 0.1$ for N_2O_5 and $\gamma = 0.01$ (upper limit) for NO_3. Uptake of NO_3 was generally negligible. The aerosol surface area could not be reliably computed from measurements aboard the DC-8 and was specified with the median value of $3\,\mu m^2\,cm^{-3}$ obtained from the companion P-3B aircraft at tropical latitudes above 6 km [*Clarke et al.,* 1999]. (*Schultz et al.* [1999] tried to estimate the aerosol surface area by correlating condensation nuclei counter measurements aboard the DC-8 with size-resolved measurements made aboard the P-3B aircraft. This approach yielded average aerosol surface areas of $\sim 24\,\mu m^2\,cm^{-3}$ above 6 km over the tropical and subtropical South Pacific which is about a factor of 10 higher than typical surface areas measured in the free troposphere (A. Clarke, personal communication, 1998). The differ-

ence could not be fully resolved.)

Table 3 gives the mean and median rates of individual reactions important in the model NO_x budget at 6-12 km altitude. There is a large budget imbalance throughout the upper troposphere, similar to previous studies. The loss rate of NO_x between 6 and 12 km surpasses the production rate by a factor of 2-3 on average. This imbalance exceeds the combined uncertainties in the measurements of NO_y species (Table1). In the lower tropical troposphere, by contrast, thermal decomposition of PAN from biomass burning sources acts as a dominant source of NO_x and the NO_x budget is balanced [*Schultz et al.*, 1999].

Figure 2 displays the model-calculated diurnally averaged ratio of chemical loss to chemical production of NO_x (L_{NO_x}/P_{NO_x}) and the NO_x lifetime versus altitude. The median L_{NO_x}/P_{NO_x} ratio is fairly constant with altitude (median 2.4, interquartile range typically 1.5–3). The NO_x lifetime increases with altitude from 2 days at 6 km to 10 days at 12 km.

If recent injection of primary NO_x in convective outflow were the major cause of the imbalance of the chemical NO_x budget, then we would expect the imbalances to be greater under conditions of high relative humidity. However, as shown in Figure 3, the L_{NO_x}/P_{NO_x} ratio tends to be largest at low relative humidity. One could invoke a scenario where injection of lightning NO_x in convective downdrafts would provide a primary source of NO_x associated with low relative humidity. Such a scenario would imply the sampling of recent outflow from very deep convection (cloud top $>$ 12 km), but kinematic back-trajectories together with infrared satellite images from PEM-Tropics A found only few occurences of these conditions. The lack of an evident dynamical explanation for the NO_x budget imbalance prompts an examination of possible chemical factors contributing to the imbalance.

3. Chemical Contributions to the NO_x Budget Imbalance

Recent laboratory measurements of the temperature-dependent rate constants for the NO_2+OH+M reaction [*Brown et al.*, 1999; *Dransfield et al.*, 1999] and the HNO_3+
OH reaction [*Brown et al.*, 1999] indicate values lower (NO_2+OH+M) and higher (HNO_3+OH) than the standard recommendations of *DeMore et al.* [1997]. A recent study of the NO_x/NO_y ratio in the lower stratosphere during polar summer [*Gao et al.*, 1999] found that using these new rate constants improves the simulated NO_x/NO_y ratio from 0.6 (with JPL-97 rates) to 0.9 times the observed ratio. For the PEM-Tropics A conditions at 6-12 km altitude, the rate constant for NO_2+OH+M is reduced by 20%, while the rate constant for HNO_3+OH is increased by 50-100% on average. The median L_{NO_x}/P_{NO_x} ratio decreases from 2.4 in the base case scenario to 2.2 using the new rate coefficients (Table 4).

Table 3 shows that hydrolysis of N_2O_5 in aerosols accounts on average for 20% of the total NO_x loss. Following the assumption commonly made in models, we assumed that the aerosol is aqueous so that N_2O_5 hydrolysis takes place [*Dentener and Crutzen*, 1993; *Lamarque et al.*, 1996; *Wang et al.*, 1998b]. *McKeen et al.* [1997] pointed out that this assumption is not necessarily correct, which has significant implications for the NO_x budget. The chemical composition of the aerosol measured during PEM-Tropics A (Figure 4) indicates full neutralization of SO_4^{2-} by NH_4^+ in 70% of all tropical samples above 6 km (Figure 5a). Laboratory studies by *Cziczo and Abbatt* [1999] for $(NH_4)_2SO_4$ and *Li-Jones et al.* [1999] for mineral dust indicate that neutral aerosols would be dry under the upper tropospheric conditions found in PEM-Tropics A (median relative humidity 25%, Table 2). *Cziczo and Abbatt* [1999] find that $(NH_4)_2SO_4$ aerosols at temperatures typical of the middle and upper troposphere (below 240 K) are dry for relative humidities below 65%, even when the energy barrier for efflorescence is taken into account. *Mozurkevich and Calvert* [1988] measured the uptake of N_2O_5 on dry $(NH_4)_2SO_4$ aerosols at 25% relative humidity and found it to be negligible ($\gamma < 0.003$).

The finding that aerosols in the upper troposphere over the South Pacific are frequently neutralized runs counter to the standard view of a background acid sulfate aerosol in the remote free troposphere [*Gilette and Blifford*, 1971; *Huebert and Lazrus*, 1980; *Whelpdale et al.*, 1987; *Dentener and Crutzen*, 1993]. Aerosol nitrate concentrations during PEM-Tropics A (Figure 4c) occasionally exceeded the ammonium present in excess of H_2SO_4 neutralization (Figure 5b), although one would not expect significant HNO_3 dissolution in acid aerosol [*Carslaw et al.*, 1995]. In these cases, neutralization of nitrate could possibly be achieved by mineral ions (e.g., Ca_2^+ or K^+) as suggested by *Tabazadeh et al.* [1998] for aerosol over the central United States. In PEM-Tropics A, mineral ion concentrations were often below the detection limit (typically 15 pmol/mol), but if we assume concentrations just below the detection limit, they would always suffice to neutralize the aerosol. Independent support for a fully neutralized aerosol over the South Pacific is offered by airborne measurements from the Aerosol Characterization Experiment (ACE-1) which indicated 50-100 pptv of gaseous NH_3 throughout the free troposphere (D. Davis, manuscript in preparation, 1999). Gaseous ammonia would be titrated

if the aerosol were acidic. A neutral aerosol would exclude the possibility of fast heterogeneous chemical conversion from HNO_3 to NO_x involving formaldehyde on acidic aerosol as proposed by *Chatfield* [1994] and *Fan et al.* [1994]. A sensitivity run without N_2O_5 (and NO_3) hydrolysis reduces median L_{NO_x}/P_{NO_x} from 2.2 (run with new rate constants) to 1.9 (Table 4).

The availability of NH_4^+ in amounts sufficient to neutralize the aerosol (Figure 4a) implies the possible presence of significant amounts of gas-phase NH_3, which could provide an additional source of NO_x via oxidation by OH [e.g., *Logan,* 1983]. According to *DeMore et al.* [1997], up to 80% of the NH_2 formed in the oxidation of NH_3 by OH would react with O_3 to form NO_x. Thus 100 pptv of NH_3 could provide a NO_x source of about $0.75\,\mathrm{pptv\,day^{-1}}$, which is 15% of the median chemical NO_x source calculated for the PEM-Tropics A conditions (Table 3). There is a need for more observations of gas-phase NH_3 and for better understanding of the mechanism of NH_3 oxidation.

While the use of new rate constants for the reactions of NO_2 and HNO_3 with OH and the possible suppression of N_2O_5 hydrolysis significantly improve the NO_x budget for PEM-Tropics A (Table 4), a median L_{NO_x}/P_{NO_x} imbalance of 1.9 persists, corresponding to a missing NO_x source of $4.3\,\mathrm{pptv\,day^{-1}}$ on average. Since the two factors discussed here increase the NO_x lifetime at 6–12 km by 30% (from 3.2 to 4.3 days; Figure 2), there is more potential for the missing source to be provided by long-range transport of primary NO_x. However, a gap in our understanding of NO_x chemistry in the free troposphere cannot be ruled out.

4. Previous Studies

A substantial body of observations for analyzing the chemical NO_x budget in the free troposphere has been presented in the literature (Table 5). Most studies report large imbalances in the NO_x budget. The reliability of the NO measurements in the experiments listed in Table 5 has been established in formal intercomparisons [*Gregory et al.*, 1990b; *Crosley,* 1996]. Aircraft measurements of NO_2 in missions prior to PEM-Tropics A had large positive biases [*Crawford et al.,* 1996]. However, most model studies in Table 5 did not use measured NO_2 but instead assumed NO_2 to be in photochemical equilibrium with NO, an assumption supported by the NO_2 measurements in PEM-Tropics A [*Schultz et al.,* 1999]. The measurement of HNO_3 appears reliable based on a recent measurement intercomparison and observed closure of the NO_y budget [*Talbot et al.,* 1999b].

The only previous studies listing average rates of individual reactions contributing to their model NO_x budget are *Fan et al.* [1994] for ABLE-3B and *Jacob et al.* [1996] for TRACE-A. The NO_x budget imbalance during ABLE-3B was small (Table 5). That study extended only to 6 km altitude; thermal decomposition of PAN was the dominant chemical source of NO_x, and N_2O_5 hydrolysis was ignored because the aerosol was fully neutralized. Therefore the effects that we investigated in section 3 would not alter the computed NO_x budget. In TRACE-A the NO_x budget imbalance at 4–12 km altitude was large (Table 5). If we suppress N_2O_5 hydrolysis and use the revised rate constants for $NO_2 + OH + M$ and $OH + HNO_3$, we find a reduction in L_{NO_x}/P_{NO_x} from 3.6 to 2.1 (4-8 km) and from 5.6 to 3.1 (8-12 km). The large effect is mainly caused by the importance of N_2O_5 hydrolysis in the *Jacob et al.* [1996] model budget which in turn is due to the high ozone concentrations observed in TRACE-A.

Global three-dimensional (3-D) models which account for long-range transport of NO_x from primary sources such as lightning and combustion also experience difficulties in simulating R_N in the upper troposphere [*Brasseur et al.,* 1996; *Wang et al.,* 1998a,b; *Lawrence and Crutzen,* 1998; *Hauglustaine et al.,* 1998; *Thakur et al.,* 1999]. These models generally achieve a good simulation of NO_x (reflecting, however, in part an adjustment of the source from lightning) but overestimate HNO_3 concentrations by a factor of 2-10 in the upper troposphere, similar to the chemical equilibrium model studies in Table 5. Aside from possible gaps in our understanding of the chemical budget of NO_x, other factors could contribute to the overestimates of HNO_3 in the 3-D models. One factor would be the fractionation of HNO_3 into aerosol nitrate (NO_3^-), which is not resolved by the models [*Wang et al.,* 1998b; *Tabazadeh et al.,* 1998]. However, during PEM-Tropics A, the NO_3^-/HNO_3 concentration ratio was usually < 0.2 (Figure 1f). Another factor would be insufficient precipitation scavenging in the free troposphere [*Wang et al.,* 1998b]. *Lawrence and Crutzen* [1998] proposed that gravitational settling of cirrus ice crystals,
not accounted for in global models, can reduce HNO_3 by a factor of 10 in the tropical upper troposphere while the impact on zonally averaged NO_x concentrations typically remains $< 20\%$.

5. Summary and Conclusions

The chemical NO_x budget in the middle and upper troposphere over the remote tropical South Pacific during PEM-Tropics A was examined with model calcula-

tions using concurrent measurements of NO, HNO_3, and PAN as constraints. A standard calculation yields a median factor of 2.4 excess of chemical loss of NO_x (conversion to HNO_3 and PAN) relative to chemical production (recycling from HNO_3 and PAN), corresponding to a missing NO_x source of about $12\,\mathrm{pptv\,day^{-1}}$. This imbalance is reduced by 10% when the recently remeasured temperature- and pressure-dependent reaction rate constants for $OH + NO_2 + M$ [*Brown et al.*, 1999; *Dransfield et al.*, 1999] and $OH + HNO_3$ [*Brown et al.*, 1999] are incorporated in the chemical mechanism.

The bulk aerosol chemical composition measured in PEM-Tropics A at 6-12 km altitude indicates in most cases total H_2SO_4 neutralization by NH_3. This observation, combined with the low relative humidities measured in PEM-Tropics A (median 25% relative to ice), suggests that the aerosol should be present in the solid phase. Suppression of N_2O_5 hydrolysis in the model improves the chemical NO_x budget imbalance in PEM-Tropics A by another 15%. Further study of the composition and phase of free tropospheric aerosols is evidently needed.

The observation of 50-100 pptv of gas-phase NH_3 in the free troposphere over the Pacific (D. Davis et al., manuscript in preparation, 1999) is inconsistent with global models [e.g., *Dentener and Crutzen*, 1994] and invites speculation about a potential NO_x source from NH_3 oxidation. For PEM-Tropics A, we derive an upper limit of 15% of the total NO_x source from this process.

If the results from this paper are applied to previous studies, reductions of the chemical NO_x budget imbalance of up to 40% are expected. The new rate constants and the possibly suppressed nighttime sink of NO_x would bring most studies into a L_{NO_x}/P_{NO_x} range of 2–3.

Acknowledgments. We would like to thank D. Davis, J. Prospero, N. Donahue, and R. Ravishankara for providing us with material that was not published before submission of this paper and B. Huebert and A. Clarke for helpful discussions on free tropospheric aerosols. L. Jaeglé deserves acknowledgement for technical support of the model calculations and helpful discussions. PEM-Tropics was funded as part of the NASA GTE program. M. Schultz acknowledges support by the Deutsche Forschungsgemeinschaft (DFG).

References

Atkinson R., D. L. Baulch, R. A. Cox, R. F. Hampson, J. A. Kerr, M. J. Rossi, and J. Troe, Evaluated kinetic and photochemical data for atmospheric chemistry - Supplement VI, *J. Phys. Chem. Ref. Data, 26*(6), 1329–1499, 1997.

Bradshaw, J. D., M. O. Rodgers, S. T. Sandholm, S. KeSheng, and D. D. Davis, A two-photon laser-induced fluorescence field instrument for ground-based and airborne measurements of atmospheric NO, *J. Geophys. Res., 90*(D7), 12,861–12,873, 1985.

Brasseur, G. P., D. A. Hauglustaine, and S. Walters, Chemical compounds in the remote Pacific troposphere: comparison between MLOPEX measurements and chemical transport model calculations, *J. Geophys. Res., 101*(D9), 14,795–14,813, 1996.

Brown, S. S., T. Gierczak, R. W. Portmann, R. K. Talukdar, J. B. Burkholder, and A.R. Ravishankara, Role of nitrogen oxides in the lower stratosphere: A reevaluation based on laboratory studies, *Geophys. Res. Lett.*, , *26*, 2387–2390, 1999.

Carslaw, K. S., S. L. Clegg, and P. Brimblecombe, A thermodynamic model of the system HCl-HNO_3-H_2SO_4-H_2Oincluding solubilities of HBr, from $<$200 to 328 K, *J. Phys. Chem., 99*, 11,557–11,574, 1995.

Chatfield, R. B., Anomalous HNO_3/NO_x ratio of remote tropospheric air: Conversion of nitric acid to formic acid and NO_x?, *Geophys. Res. Lett., 21*, 2705–2708, 1994.

Clarke, A. D., F. Eisele, V. N. Kapustin, K. Moore, R. Tanner, L. Mauldin, M. Litchy, B. Lienert, M. A. Carroll, and G. Albercook, Nucleation in the equatorial free troposphere: Favorable environments during PEM-Tropics, *J. Geophys. Res., 104*(D5), 5735–5744, 1999.

Crawford, J., et al., Photostationary state analysis of the NO_2-NO system based on airborne observations from the western and central north Pacific, *J. Geophys. Res., 101*, 2053–2072, 1996.

Crawford, J. H., et al., Implications of large scale shifts in tropospheric NO_x levels in the remote tropical Pacific, *J. Geophys. Res., 102*(D23), 28,447–28,468, 1997.

Crosley, D. R., The NO_y blue ribbon panel, *J. Geophys. Res., 101*(D1), 2049–2052, 1996.

Cziczo, D. J., and J. P. D. Abbatt, Deliquescence, effluorescence and supercooling of ammonium sulfate aerosols at low temperature: Implications for cirrus cloud formation and aerosol phase in the atmosphere, *J. Geophys. Res., 104*(D11), 13,781–13,790, 1999.

Davis, D. D., et al., Assessment of ozone photochemistry in the western North Pacific as inferred from PEM-West A observations during the fall 1991, *J. Geophys. Res., 101*(D1), 2111–2134, 1996.

DeMore, W. B., S. P. Sander, D. M. Golden, R. F. Hampson, M. J. Kurylo, C. J. Howard, A. R. Ravishankara, C. E. Kolb, and M. J. Molina, Chemical kinetics and photochemical data for use in stratospheric modeling, *JPL Pub., 97-4*, 1997.

Dentener, F. J., and P. J. Crutzen, Reaction of N_2O_5 on tropospheric aerosols: Impact on the global distributions of NO_x, O_3, and OH, *J. Geophys. Res., 98*(D4), 7149–7162, 1993.

Dentener, F. J., and P. J. Crutzen, A three-dimensional model of the global ammonia cycle, *J. Atmos. Chem.*, *19*, 331–369, 1994.

Dibb, J. E., R. W. Talbot, E. M. Scheuer, D. R. Blake, N. J. Blake, G. L. Gregory, G. W. Sachse, and D. C. Thornton, Aerosol chemical composition and distribution during the Pacific Exploratory Mission - Tropics, *J. Geophys. Res.*, *104*(D5), 5785–5800, 1999.

Dransfield, T. J., K. K. Perkins, N. M. Donahue, J. G. Anderson, M. M. Sprengnether, and K.L. Demerjian, Temperature and pressure dependent kinetics of the gas-phase reaction of the hydroxyl radical with nitrogen dioxide, *Geophys. Res. Lett.*, *26*(6), 687–690, 1999.

Fan, S.-M., D. J. Jacob, D. L. Mauzerall, J. D. Bradshaw, S. T. Sandholm, D. R. Blake, H.B. Singh, R. W. Talbot, G. L. Gregory, and G. W. Sachse, Origin of tropospheric NO_x over subarctic eastern Canda in summer, *J. Geophys. Res.*, *99*(D8), 16,867–16,877, 1994.

Gao, R. S., et al., A comparison of observations and model simulations of NO_x/NO_y in the lower stratosphere, *Geophys. Res. Lett.*, *26*(8), 1153–1156, 1999.

Gierczak, T., J. B. Burkholder, S. Bauerle, and A. R. Ravishankara, Photochemistry of acetone under tropospheric conditions, *J. Chem. Phys.*, *231*(2-3), 229–244, 1998.

Gillette, D. A., and I. H. Blifford Jr., Composition of tropospheric aerosols as a function of altitude, *J. Atmos. Sci.*, *28*, 1199–1210, 1971.

Gregory, G. L., J. H. Hoell, B. A. Ridley, H. B. Singh, B. Gandrud, L. J. Salas, and J. Shetter, An intercomparison of airborne PAN measurements, *J. Geophys. Res.*, *95*(D7), 10,077–10,087, 1990a.

Gregory, G. L., J. M. Hoell Jr., A. L. Torres, M. A. Carroll, B. A. Ridley, M. O. Rodgers, J. Bradshaw, S. Sandholm, and D. D. Davis, An intercomparison of airborne nitric oxide measurements: A second opportunity, *J. Geophys. Res.*, *95*(D7), 10,129–10,138, 1990b.

Hauglustaine, D. A., B. A. Ridley, S. Solomon, P. G. Hess, and S. Madronich, HNO_3/NO_x ratio in the remote troposphere during MLOPEX 2: Evidence for nitric acid reduction on carbonaceous aerosols, *Geophys. Res. Lett.*, *23*(19), 2609–2612, 1996.

Hauglustaine, D. A., G. P. Brasseur, S. Walters, P. J. Rasch, J. F. Müller, L. K. Emmons, and M. A. Carroll, MOZART, a global chemical transport model for ozone and related chemical tracers, 2: Model results and evaluation, *J. Geophys. Res.*, *103*(D21), 28,291–28,335, 1998.

Hoell, J. M., D. D. Davis, D. J. Jacob, M. O. Rodgers, R. E. Newell, H. E. Fuelberg, R. J. McNeal, J. L. Raper, and R. J. Bendura, The Pacific Exploratory Mission in the Tropical Pacific: PEM-Tropics A, August-September 1996, *J. Geophys. Res.*, *104*(D5), 5567–5584, 1999.

Huebert, B. J., and A. L. Lazrus, Bulk composition of aerosols in the remote atmosphere, *J. Geophys. Res.*, *85*, 7337–7344, 1980.

Jacob, D. J., Heterogeneous chemistry and tropospheric ozone, *Atmos. Environ.*, in press 1999.

Jacob, D. J., et al., Summertime photochemistry of the troposphere at high northern latitudes, *J. Geophys. Res.*, *97*(D15), 16,421–16,431, 1992.

Jacob, D. J., et al., Origin of ozone and NO_x in the tropical troposphere: A photochemical analysis of aircraft observations over the South Atlantic basin, *J. Geophys. Res.*, *101*(D19), 24,235–24,250, 1996.

Jaeglé, L., D. J. Jacob, Y. Wang, A. J. Weinheimer, B. A. Ridley, T. L. Campos, G. W. Sachse, and D. Hagen, Sources and chemistry of NO_x in the upper troposphere over the central United States, *Geophys. Res. Lett.*, *25*(10), 1705–1708, 1998.

Kawakami, S., et al., Impact of lightning and convection on reactive nitrogen in the tropical free troposphere, *J. Geophys. Res.*, *102*(D23), 28,367–28,384, 1997.

Kondo, Y., M. Koike, S. Kawakami, H. B. Singh, H. Nakajima, G. L. Gregory, D. R. Blake, G. W. Sachse, J. T. Merrill, and R. E. Newell, Profiles and partitioning of reactive nitrogen over the Pacific ocean in winter and early spring, *J. Geophys. Res.*, *102*(D23), 28,405–28,424, 1997.

Lamarque, J.-F., G. P. Brasseur, P. G. Hess, and J.-F. Müller, Three-dimensional study of the relative contributions of the different nitrogen sources in the troposphere, *J. Geophys. Res.*, *101*(D17), 22,955–22,968, 1996.

Lary, D. J., A. M. Lee, R. Toumi, M. J. Newchurch, M. Pirre, and J. B. Renard, Carbon aerosols and atmospheric photochemistry, *J. Geophys. Res.*, *102*(D3), 3671–3682, 1997.

Lawrence, M. G., and P. J. Crutzen, The impact of cloud particle gravitational settling on soluble trace gas distributions, *Tellus , Ser. B*, *50*(3), 263–289, 1998.

Li-Jones, X., H. B. Maring, and J. M. Prospero, Effect of relative humidity on light-scattering by mineral dust aerosol as measured in the marine boundary layer over the tropical Atlantic ocean, *J. Geophys. Res.*, *103*(D23), 31,113–31,121, 1998.

Liu, S. C., et al., A study of the photochemistry and ozone budget during the Mauna Loa Observatory Photochemistry Experiment, *J. Geophys. Res.*, *97*(D10), 10,463–10,471, 1992.

Liu, S. C., et al., Model study of tropospheric trace species distributions during PEM-West A, *J. Geophys. Res.*, *101*(D1), 2073–2086, 1996.

Logan, J. A., Nitrogen-oxides in the troposphere: Global and regional budgets, *J. Geophys. Res.*, *88*(C15), 785–807, 1983.

McKeen, S. A., T. Gierczak, J. B. Burkholder, P. O. Wennberg, T. F. Hanisco, E. R. Keim, R.-S. Gao, S. C. Liu, A. R. Ravishankara, and D. W Fahey, The photochemistry of acetone in the upper troposphere: A source of odd-hydrogen radicals, *Geophys. Res. Lett.*, *24*(24), 3177–3180, 1997.

Mozurkewich, M., and J. G. Calvert, Reaction probability of N_2O_5 on aqueous aerosols, *J. Geophys. Res.*, *93*(D12), 15,889–15,896, 1988.

Prather, M. J., and D. J. Jacob, A persistent imbalance in HO_x and NO_x photochemistry of the upper troposphere driven by deep tropical convection, *Geophys. Res. Lett.*, *24*(24), 3189–3192, 1997.

Sandholm, S. T., J. D. Bradshaw, K. S. Dorris, M. O. Rodgers, and D. D. Davis, An airborne compatible photofragmen-

tation two-photon laser-induced fluorescence instrument for measuring background tropospheric levels of NO, NO_x, and NO_2, *J. Geophys. Res.*, *95*(D7), 10,155–10,161, 1990.

Sandholm, S., et al., Summertime partitioning and budget of NO_y compounds in the troposphere over Alaska and Canada: ABLE 3B, *J. Geophys. Res.*, *99*(D1), 1837–1861, 1994.

Sandholm, S., S. Smyth, R. Bai, and J. Bradshaw, Recent and future improvements in two-photon laser-induced-fluorescence NO measurement capabilities, *J. Geophys. Res.*, *102*(D23), 28,651–28,663, 1997.

Schultz, M., R. Schmitt, K. Thomas, and A. Volz-Thomas, Photochemical box modeling of long-range transport from North America to Tenerife during the North Atlantic Regional Experiment (NARE) 1993, *J. Geophys. Res.*, *103*(D11), 13,477–13,488, 1998.

Schultz, M. G., et al., On the origin of tropospheric ozone and NO_x over the tropical South Pacific, *J. Geophys. Res.*, *104*(D5), 5829–5844, 1999.

Singh, H. B., and L. J. Salas, Methodology for the analysis of peroxyacetylnitrate (PAN) in the unpolluted atmosphere, *Atmos. Environ.*, *17*, 1507–1516, 1983.

Singh, H. B., M. Kanakidou, P. J. Crutzen, and D. J. Jacob, High concentrations and photochemical fate of oxygenated hydrocarbons in the global troposphere, *Nature*, *378*, 50–54, 1995.

Singh, H. B., et al., Reactive nitrogen and ozone over the western Pacific: Distribution, paritioning, and sources, *J. Geophys. Res.*, *101*(D1), 1793–1808, 1996a.

Singh, H. B., et al., Impact of biomass burning emissions on the composition of the South Atlantic troposphere: Reactive nitrogen and ozone, *J. Geophys. Res.*, *101*(D19), 24,203–24,220, 1996b.

Singh, H. B., et al., Latitudinal distribution of reactive nitrogen in the free troposphere over the Pacific ocean in late winter early spring, *J. Geophys. Res.*, *103*(D21), 28,237–28,246, 1998.

Smyth, S. B., et al., Factors influencing the upper free tropospheric distribution of reactive nitrogen over the South Atlantic during the TRACE-A experiment, *J. Geophys. Res.*, *101*(D19), 24,165–24,186, 1996.

Tabazadeh, A., M. Z. Jacobson, H. B. Singh, O. B. Toon, J. S. Lin, R. B. Chatfield, A. N. Thakur, R. W. Talbot, and J. E. Dibb, Nitric acid scavenging by mineral and biomass aerosols, *Geophys. Res. Lett.*, *25*(22), 4185–4188, 1998.

Talbot, R. W., K. M. Beecher, R. C. Hariss, and W. R. Cofer III, Atmospheric geochemistry of formic and acedic acids at a mid-latitude temperate site, *J. Geophys. Res.*, *93*(D2), 1638–1652, 1988.

Talbot, R. W., A. S. Vijgen, and R. C. Harriss, Measuring tropospheric HNO_3: Problems and prospects for nylon filter and mist chamber techniques, *J. Geophys. Res.*, *95*(D6), 7553–7561, 1990.

Talbot, R. W., et al., Large-scale distributions of tropospheric nitric, formic, and acetic acids over the western Pacific basin during wintertime, *J. Geophys. Res.*, *102*(D23), 28,303–28,313, 1997.

Talbot, R. W., J. E. Dibb, E. M. Scheuer, D. R. Blake, N. J. Blake, G. L. Gregory, G. W. Sachse, J. D. Bradshaw, S. T. Sandholm, and H. B. Singh, Influence of biomass combustion emissions on the distribution of acidic trace gases over the southern Pacific basin during austral springtime, *J. Geophys. Res.*, *104*(D5), 5623–5634, 1999a.

Talbot, R. W., et al., Reactive nitrogen budget during the NASA SONEX mission, *Geophys. Res. Lett.*, *26*(20), 3057–3060, 1999b.

Thakur, A. N., H. B. Singh, P. Mariani, Y. Chen, Y. Wang, D. J. Jacob, G. Brasseur, J. F. Müller, and M. Lawrence, Distribution of reactive nitrogen species in the remote free troposphere: Data and model comparisons, *Atmos. Environ.*, *33*(9), 1403–1422, 1999.

Wang, Y., D. J. Jacob, and J. A. Logan, Global simulation of tropospheric O_3-NO_x-hydrocarbon chemistry: 1. Model formulation, *J. Geophys. Res.*, *103*(D9), 10,713–10,726, 1998a.

Wang, Y., J. A. Logan, and D. J. Jacob, Global simulation of tropospheric O_3-NO_x-hydrocarbon chemistry: 2. Model evaluation and global ozone budget, *J. Geophys. Res.*, *103*(D9), 10,727–10,756, 1998b.

Whelpdale, D. M., W. C. Keene, A. D. A. Hanssen, and J. Boatman, Aircraft measurements of sulfur, nitrogen, and carbon species during WATOX-86, *Global Biogeochem. Cycles*, *1*, 357–368, 1987.

J. E. Dibb and R. W. Talbot, Institute for the Study of Earth, Oceans, and Space, University of New Hampshire, Durham, NH 03824.

D. J. Jacob, Division of Engineering and Applied Sciences and Department of Earth and Planetary Sciences, Harvard University, 29 Oxford St., Cambridge, MA 02139. (djj@io.harvard.edu)

S. T. Sandholm, School of Earth and Atmospheric Sciences, Georgia Institute of Technology, Atlanta, GA 30332.

M. G. Schultz, Max-Planck-Institut für Meteorologie, Bundesstr. 55, 20146 Hamburg, Germany. (martin.schultz@dkrz.de)

H. B. Singh, NASA Ames Research Center, Moffett Field, CA 94035.

Received January 22, 1999; revised September 16, 1999; accepted September 23, 1999.

[1] Division of Engineering and Applied Sciences and Department of Earth and Planetary Sciences, Harvard University, Cambridge, Massachusetts.

[2] Now at Max-Planck-Institut für Meteorologie, Hamburg, Germany.

[3] Deceased June 16, 1997.

[4] School of Earth and Atmospheric Sciences, Georgia Institute of Technology, Atlanta.

[5] Institute for the Study of Earth, Oceans, and Space, University of New Hampshire, Durham.

[6] NASA Ames Research Center, Moffett Field, California.

This preprint was prepared with AGU's LaTeX macros v5.01. File pemtnox04 formatted March 22, 2000.

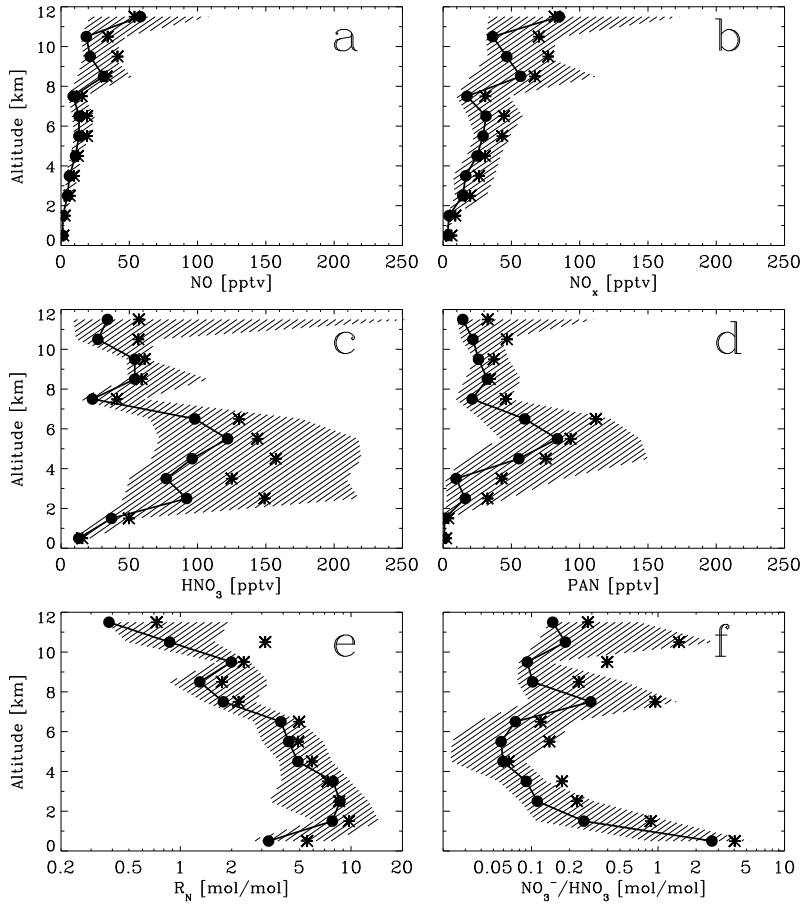

Figure 1. Vertical profiles of (a) NO, (b) NO_x (= $\mathrm{NO} + \mathrm{NO}_2 + \mathrm{NO}_3 + 2\,\mathrm{N}_2\mathrm{O}_5 + \mathrm{HNO}_2 + \mathrm{HO}_2\mathrm{NO}_2$), (c) gas-phase HNO_3, and (d) PAN concentrations as well as (e) the $\mathrm{HNO}_3/(\mathrm{NO} + \mathrm{NO}_2)$ ratio (R_N) and (f) the ratio of aerosol NO_3^- to gas-phase HNO_3 concentrations. Concentrations of NO, PAN, HNO_3 and NO_3^- are aircraft measurements from PEM-Tropics A (0–30°S, 165°E–105°W). Concentrations of NO_x species other than NO are photochemical model values. NO data are displayed for zenith angles $< 60°$ only. Circles are median values over 1 km altitude bands, stars denote means, and the shaded areas span the interquartile ranges. NO_3^- values below the limit of detection (LOD) are set to $1/2 \times \mathrm{LOD}$ for Figure 1f.

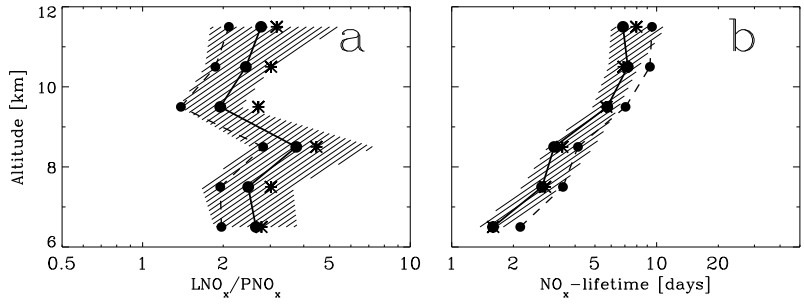

Figure 2. Vertical profiles of (a) the ratio of 24-hour averaged rates of chemical loss to chemical production of NO_x and (b) the chemical lifetime of NO_x. Values are results from standard steady state point model calculations for the ensemble of data summarized in Figure 1. Circles are medians over 1 km altitude bands, stars are means, and the shaded areas span the interquartile ranges from the standard simulation. The dashed line shows results for a simulation with new rate constants for $NO_2 + OH + M$ [*Brown et al.,* 1999; *Dransfield et al.,* 1999] and $HNO_3 + OH$ [*Brown et al.,* 1999] and without N_2O_5 hydrolysis.

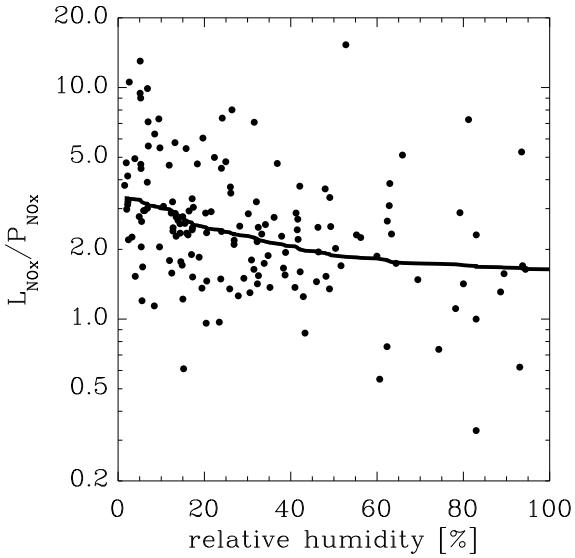

Figure 3. Ratio of chemical loss to production of NO_x for the data in Figure 1, plotted versus relative humidity with respect to ice. Loss and production rates of NO_x are from the standard simulation. Dots represent the individual calculations; the line is a smoothed running geometric average.

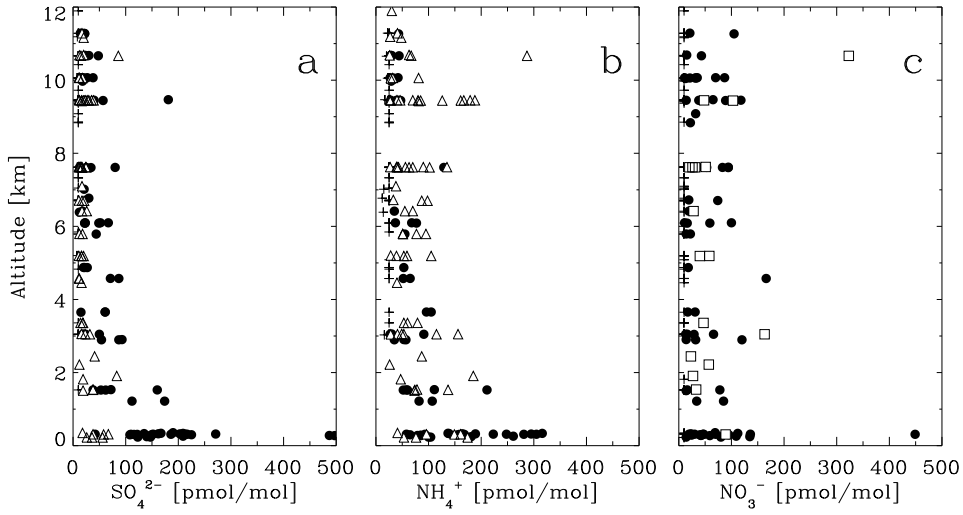

Figure 4. Vertical profiles of aerosol composition during PEM-Tropics A (0-30°S, 165°E-105°W, 6-12 km): (a) sulfate, (b) ammonium, (c) nitrate. Open triangles in Figures 4a and 4b denote samples where H_2SO_4 is fully neutralized by NH_3 ($[NH_4^+] > 2[SO_4^{2-}]$). Open squares in Figure 4c denote samples where HNO_3 titrates the excess NH_4^+ ($[NH_4^+] > 2[SO_4^{2-}]$ and $[NO_3^-] > [NH_4^+] - 2[SO_4^{2-}]$). Plusses show data below detection limit (LOD) (set to $1 \times$ LOD for display). Closed symbols represent all other points, including those where diagnosis of the NH_4^+- SO_4^{2-}-NO_3^- balance could not be conducted due to concentrations below the detection limit.

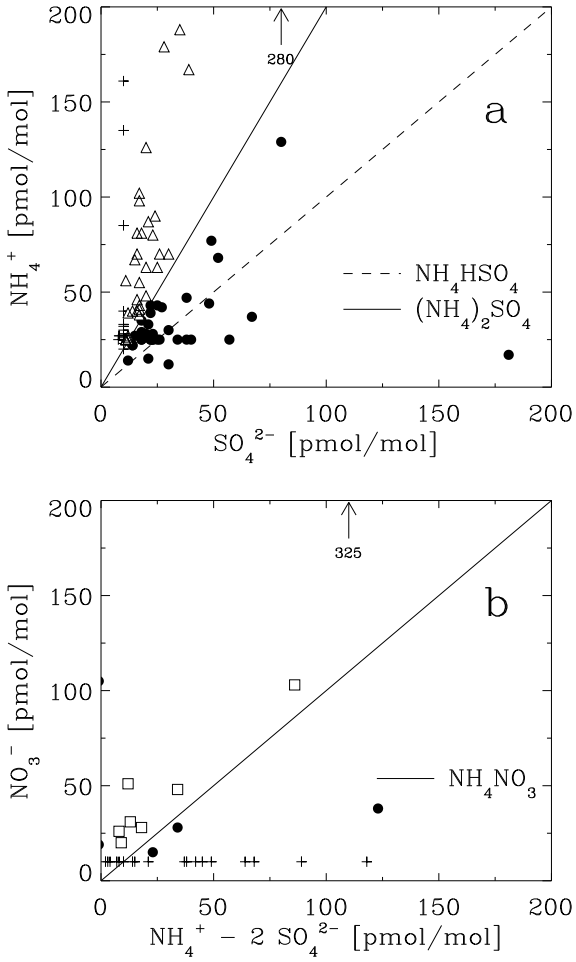

Figure 5. Relationships at 6-12 km between (a) aerosol sulfate and ammonium and (b) aerosol nitrate and ammonium in excess of sulfate. The dashed line in Figure 5a is the 1:1 line; the solid line is the 2:1 line. The solid line in Figure 5b is the 1:1 line. Symbols are the same as in Figure 4.

Table 1. Instrument Parameters for Key Measurements During PEM-Tropics A

Species	Technique	Limit of Detection	Accuracy, %	PI[a]
NO	TP-LIF	$< 0.4\,\mathrm{pptv}$	13	J. Bradshaw
NO_2	photolysis, TP-LIF	$0.5 - 11\,\mathrm{pptv}$	$25 - 40$	J. Bradshaw
HNO_3	mist chamber	$< 20\,\mathrm{pptv}$	$15 - 20\ (> 25\,\mathrm{pptv})$	R. Talbot
particulate NO_3^-	filter sampling/ion chromatography	$10\,\mathrm{pmol/mol}$	20	R. Talbot
PAN	GC/ECD	$1\,\mathrm{pptv}$	20	H. Singh
J(NO_2)[b]	4π spectrometer	$4 \cdot 10^{-7}\,\mathrm{s}^{-1}$	12	R. Shetter

TP-LIF, two photon-laser induced fluorescence; GC/ECD, gas chromatography with electron capture detector; pptv, parts per trillion by volume.

[a] Principal Investigator.

[b] Photolysis frequency for NO_2.

Table 2. Median Airmass Composition Over the Tropical South Pacific (0-30°S, 165°E-90°W, 6-12 km)

Species	All Data ($N = 158$)	Relative Humidity[a] $< 10\%$ ($N = 33$)
Temperature, K	249 (234-256)	252 (244-260)
Potential temperature, K	336 (331-342)	335 (331-339)
relative humidity, %	25 (13-46)	5 (3-7)
NO, pptv	16 (9-31)	36 (12-60)
NO_x, pptv[b]	35 (18-63)	77 (22-141)
HNO_3, pptv	48 (23-82)	87 (41-183)
R_N, mol/mol[c]	1.9 (1.2-3.2)	1.6 (0.8-3.5)
PAN, pptv	27 (15-64)	47 (15-121)
O_3, ppbv	33 (28-49)	48 (29-80)
CO, ppbv	58 (54-65)	69 (54-85)
C_2H_2, pptv	36 (27-58)	68 (29-94)
C_2H_2/CO, pptv/ppbv	0.6 (0.5-0.8)	1.0 (0.6-1.1)
H_2O_2, pptv	372 (269-592)	322 (209-446)
CH_3OOH, pptv	212 (116-340)	114 (75-199)
HCOOH, pptv	36 (27-58)	72 (41-133)
CH_3COOH, pptv	34 (24-68)	54 (24-114)
CH_3I, pptv	0.07 (0.05-0.11)	0.05 (0.04-0.07)
NH_4^+, pmol/mol[d]	LOD (LOD-46)	27 (LOD-46)
SO_4^{2-}, pmol/mol[d]	13 (LOD-22)	16 (LOD-21)
NO_3^-, pmol/mol[d]	LOD (LOD-26)	LOD (LOD-26)

PEM-Tropics A DC-8 data. Values in parentheses are interquartile ranges.

[a] With respect to ice.

[b] $NO_x = NO + NO_2 + NO_3 + 2\,N_2O_5 + HNO_2 + HO_2NO_2$; concentrations of species other than NO are calculated from the photochemical model (standard simulation).

[c] $R_N = HNO_3/(NO + NO_2)$. NO_2 from photochemical model.

[d] Limit of detection (LOD) = 25 pmol/mol for NH_4^+ and 10 pmol/mol for SO_4^{2-} and NO_3^-.

Table 3. Mean (Median) 24-Hour Average Chemical NO_x Budget in the Upper Troposphere Over the Tropical South Pacific

Reaction	Mean (Median)
NO_x Production, $\mathrm{pptv\,d^{-1}}$	
$HNO_3 + OH$	1.9 (1.2)
$HNO_3 + h\nu$	2.0 (1.5)
$PAN + h\nu$	1.1 (0.7)
PAN thermolysis	0.4 (< 0.1)
total production	5.4 (3.6)
NO_x Loss, $\mathrm{pptv\,d^{-1}}$	
$NO_2 + OH + M$	11.6 (5.5)
$N_2O_5 + H_2O$ (aerosol)	3.4 (1.2)
$NO_2 + CH_3COO_2 + M$	2.6 (2.1)
total loss	17.6 (9.3)
NO_x Budget, ratio	
L_{NO_x}/P_{NO_x}	2.5 (2.1)

Model results for PEM-Tropics A (run 0, base case), 0-30°S, 165°E-105°W, 6-12 km altitude, with NO_x defined as $NO + NO_2 + NO_3 + 2\,N_2O_5 + HNO_2 + HO_2NO_2$; PAN formation and loss rates are corrected for internal cycling within the $[PAN + CH_3COO_2]$ family [*Jacob et al.,* 1996].

Table 4. Model Sensitivity of L_{NO_x}/P_{NO_x} and NO_x Lifetime in PEM-Tropics A

Model Run	L_{NO_x}/P_{NO_x}	NO_x Lifetime, days
Results from *Schultz et al.* [1999][a]	2.6 (1.7-3.8)	2.8 (1.7-5.6)
Standard simulation with JPL-97 rates[b]	2.4 (1.4-3.5)	3.2 (2.1-5.8)
New rate constants[c]	2.2 (1.4-3.0)	3.4 (2.2-6.5)
New rate constants and no heterogeneous NO_x loss	1.9 (1.2-2.5)	4.1 (2.5-7.7)

L_{NO_x}/P_{NO_x} is the ratio of the 24-hour averaged chemical loss rate of NO_x (L_{NO_x}) to the chemical production rate of NO_x (P_{NO_x}) calculated with a chemical point model constrained by PEM-Tropics A aircraft observations over the tropical and substropical South Pacific (0-30°S, 165°E-105°W, 6-12 km altitude). Values are medians, values in parantheses give the interquartile range.

[a] Aerosol surface area estimated from condensation nuclei counts. Median surface area too large ($24\,\mu m^2\,cm^{-3}$).

[b] N_2O_5 hydrolysis with $\gamma = 0.1$; water vapor and peroxide concentrations as observed. Aerosol surface area = $3\,\mu m^2\,cm^{-3}$.

[c] Revised temperature dependent rate constants for $NO_2 + OH + M$ [*Dransfield et al.*, 1999] and $HNO_3 + OH$ [*Brown et al.*, 1999]. All other parameters as in standard simulation.